

## Observation of Electron-Ion Instability in Counterstreaming Ion Beams and Plasma System

Y. Nakamura, Y. Nomura, and T. Itoh

*Institute of Space and Aeronautical Science, University of Tokyo, Komaba, Meguro-ku, Tokyo, Japan*

(Received 10 June 1977)

Instabilities in a triple-plasma device which produces counterstreaming ion beams are investigated. We observed a new type of standing oscillations whose wavelength is given by  $D/n$ , where  $D$  is the distance between boundaries and  $n$  is an integer. The phase velocity and the critical beam velocity are compared with theory.

Theoretical studies of the interaction of an ion beam with a nonmagnetized plasma predict that the ion beam causes instabilities.<sup>1</sup> These instabilities are classified into the ion-ion and the electron-ion instability. In the former case in which  $V_b \approx C_s$ , where  $V_b$  and  $C_s$  are the base velocity and the ion acoustic speed, respectively, the ion acoustic wave couples with the slow space-charge wave of the beam. Spatially growing test waves due to the instability have been observed experimentally.<sup>2</sup> In the latter case in which  $V_b \geq 3C_s$ , the instability which is derived not from the fluid theory but from the kinetic theory has not been observed yet. In this Letter, observation of the electron-ion instability in counterstreaming ion beams and plasma system is reported.

The experiment was performed using a magnetic multipole<sup>3</sup> triple-plasma device of 40 cm in diameter and 1 m in length shown schematically in Fig. 1. The device was separated into a target and two source chambers by floating grids ( $G$ ) of 20 meshes per inch made of 0.1-mm molybdenum wires. The distance between the grids was 17.2 cm. The system was evacuated down to  $0.5 \mu\text{Torr}$  and was operated at a pressure of 0.05 to 0.1 mTorr in argon. In the source chambers aluminum rectangular pipes (2 cm width and 2.5 cm spacing) enclosing permanent magnets inside were

used as the anode for the discharge from a set of tungsten filaments ( $F$ ). The discharge voltage was 40 V and the discharge current was 10–200 mA. In the target chamber, aluminum pipes were grounded. The ion energy distribution was obtained by movable retarding analyzers of 1 cm in diameter which consisted of two grids and a collector plate. Steady streams of ions flew from the source chambers into the target chamber when the anode potential ( $V_a$ ) of the source chambers was raised, and a triple-humped ion energy distribution was observed in the target chamber by two energy analyzers. Though there was no discharge in the target chamber, a plasma was generated there by some primary electrons which went through the grids. The oscillations were detected by monitoring electron saturation current to a movable 0.2-mm-diam and 2-cm-long cylindrical probe. Test waves were excited by applying a small sinusoidal signal (0.1 V, peak to peak) to the grid through a capacitor and the propagation patterns were obtained by usual interferometer technique.

We increased the beam velocity from zero, keeping the velocity and the density of both beams equal. Plasma parameters which depend on  $V_b$  are tabulated in Fig. 2. The temperature ratio  $T_e/T_i$  was 10 and the temperature and density of electrons were 1.5 eV and about  $4 \times 10^7 \text{ cm}^{-3}$ , respectively. When  $0 \leq V_b/C_s < 0.9$ , test waves whose frequency was smaller than 100 kHz damped spatially. When  $0.9 \leq V_b/C_s \leq 2$ , it was found that for low frequencies the test wave grew spatially. The phase velocity of the unstable wave was independent of the frequency. For frequencies near or greater than the ion plasma frequency, only the fast beam mode was observed. These phenomena are similar to those reported in Ref. 2. When  $2 < V_b/C_s < 3$ , for low frequencies both ion acoustic wave and fast beam mode were transmitted; for frequencies near or greater than the ion plasma frequency, only the fast beam mode propagated. The phase velocities of those test waves mentioned above did not depend on the fre-

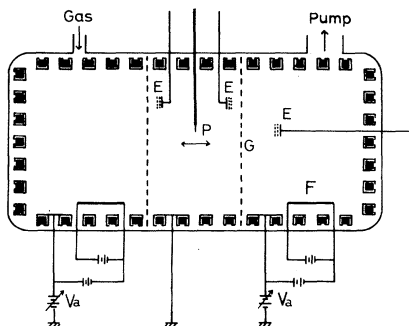


FIG. 1. Schematic diagram of experimental setup. Closed squares show permanent magnets.

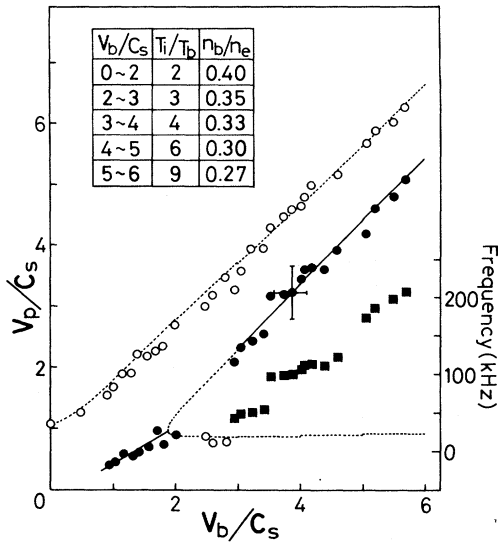


FIG. 2. Phase velocities and frequencies as a function of ion beam velocity. Velocities are normalized with  $C_s$ . Closed squares show frequencies of standing oscillation. Open circles and closed circles are phase velocities of stable and unstable wave, respectively. Solid and dotted curves correspond to the theoretical phase velocities of the unstable and stable modes, respectively. Table gives experimental parameters as a function of beam velocity.

quency and are shown by solid and open circles for unstable and stable waves, respectively, in Fig. 2 as a function of beam velocity ( $0 \leq V_b/C_s < 3$ ). At  $V_b/C_s \approx 3.0$ , an oscillation whose frequency and spectrum width are 44.2 kHz and about 1 kHz, respectively, appeared spontaneously. As  $V_b$  was increased further, the frequency of the oscillations changed discontinuously as shown by solid squares in Fig. 2. It suggests that the oscillations are standing waves and that the frequency jump is due to the change of mode number. To confirm it, the signal picked up by the movable probe was fed into a spectrum analyzer and the axial variation of the amplitude was measured.

Some raw data for different beam velocities are shown in Fig. 3. Correlation measurement by the grid and the probe revealed that the phase of an amplitude peak in Fig. 3 jumped by  $\pi$  from adjacent peaks. The results clearly show that the oscillations excited spontaneously are standing oscillations. Amplitude patterns of Fig. 3 show that there are antinodes at the boundaries, that is, the wave reflected there is in phase with the incident one.<sup>4</sup> Antinodes at boundaries have been also observed in the case of oscillations in

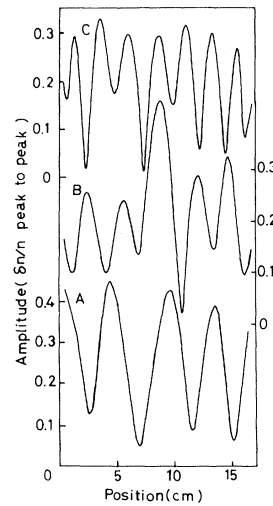


FIG. 3. Amplitude patterns of the standing oscillations. (a) Frequency is 48.5 kHz,  $n=2$ , and  $V_b/C_s = 3.05$ ; (b) frequency is 99.2 kHz,  $n=3$ , and  $V_b/C_s = 4.05$ ; (c) frequency is 186 kHz,  $n=4$ , and  $V_b/C_s = 5.2$ .

counterstreaming electron beams.<sup>5</sup> To confirm the in-phase reflection, the time-of-flight method was made. A test pulse which was transmitted by one grid propagated toward the other grid and reflected in phase. The wavelength of the oscillation is nearly given by  $D/n$ , where  $D$  is the distance between the grids and  $n$  is an integer. It indicates that the phase of the oscillation at both boundaries is equal at a given time. It was confirmed by observing two signals from the grids on an oscilloscope. A direct coupling which causes feedback between boundaries makes the phases at boundaries equal. This kind of in-phase coupling has been already observed in current-driven and ion-beam-excited ion acoustic waves.<sup>6</sup> In the electron oscillation,<sup>5</sup> there is no direct coupling between boundaries so that the wavelength of the oscillation is given by  $2D/n$ .

We obtained the phase velocity of the spontaneous oscillation by multiplying its frequency with the wavelength estimated from its amplitude pattern like those shown in Fig. 3. The phase velocities are shown by closed circles in Fig. 2 as a function of  $V_b/C_s$  ( $\geq 3$ ). The result shows that the unstable standing oscillations are the slow beam mode. The phase velocity of the fast beam mode was measured from the interferometer output of the test wave whose frequency was 1 to 3 times larger than the ion plasma frequency and is shown by open circles in Fig. 2.

When the counterstreaming ion beams of den-

sity  $n_b$ , with a drifting Maxwellian distribution (mean velocity  $V_b$  and temperature  $T_b$ ) are introduced into a plasma with stationary ions (with density  $n_i$ , at temperature  $T_i$ ) and electrons (with density  $n_e = 2n_b + n_i$ , at temperature  $T_e$ ), the kinetic dispersion relation can be written as

$$k^2 = \frac{k_a^2}{2} Z' \left( \frac{\omega}{ka_e} \right) + \frac{k_i^2}{2} Z' \left( \frac{\omega}{ka_i} \right) + \frac{k_b^2}{2} Z' \left( \frac{\omega - kV_b}{ka_b} \right) + \frac{k_b^2}{2} Z' \left( \frac{\omega + kV_b}{ka_b} \right), \quad (1)$$

where  $k_j^2 = 4\pi n_j e^2 / T_j$ ,  $a_j^2 = 2T_j / m_j$ ,  $Z$  is the plasma dispersion function and the subscripts  $e$ ,  $i$ , and  $b$  are for electrons, background ions, and beam ions, respectively. A complex  $\omega (= \omega_r + i\omega_i)$  is obtained numerically from Eq. (1) for real  $k$  under the experimental parameters. For the ion-ion instability, as  $\omega_r/k \approx C_s$ , the Landau damping caused by plasma ions is largest and it is overcome by the Landau growth caused by beam ions. For the electron-ion instability, as  $\omega_r/k \approx 2.5C_s$ , not only the imaginary part but also the real part of the plasma-ion term of Eq. (1) is much smaller than the electron term so that electrons couple with beam ions.

As for the spontaneous oscillation, we changed twice as many as its frequency by varying the distance between the grids and knew the wavelength from the amplitude pattern. The obtained phase velocity does not depend on the frequency. Therefore, the dispersion of all the modes was experimentally linear. Since the experimental  $k^2$  is much smaller than  $k_e^2$ , it agrees with the dispersion obtained from Eq. (1). The phase velocities of principal modes calculated from Eq. (1) are shown in Fig. 2 by dotted curves ( $\omega_i < 0$ ) and solid lines ( $\omega_i > 0$ ) as a function of  $V_b/C_s$ . Here, plasma parameters listed in Fig. 2 and  $T_e = 10T_i$  are used. We substitute  $0.01k_e^2$  for  $k^2$ , since  $k$  of the oscillation when  $V_b/C_s \approx 3$  is  $0.1k_e$  and since it is small enough for the condition that  $k^2/k_e^2 \ll 1$  to hold. The unstable regions  $0.8 < V_b/C_s < 2$  and  $V_b/C_s \geq 3$  correspond to the ion-ion and the electron-ion instability, respectively. When  $\omega_r/k \approx V_b \gg a_i, a_b$  and  $k \ll k_e$ , the phase velocities of beam modes  $\omega_r/k \approx V_b \pm C_s(n_b/n_e)^{1/2}$  which are easily obtained from Eq. (1). The phase velocity of stable ion-acoustic mode is about  $C_s(n_i/n_e)^{1/2} \times (1 + 3T_i n_e / T_e n_i)^{1/2}$  under the condition  $a_b \ll a_i \ll \omega_r/k \ll V_b \ll a_e$ .

When  $V_b$  increases, the mode number  $n$  or  $k$  ( $= 2\pi n/D$ ) of the oscillation increases as shown in Fig. 3. The reason is that the estimated  $k_m$  which gives maximum growth rate increases with  $V_b$ . When  $V_b/C_s = 4$ ,  $k_m/k_e = 0.16$ , which agrees with the observed  $k/k_e$  ( $= 0.15$ ). Agreement between the experimental and theoretical results shows that the oscillations are excited by the

electron-ion instability. It should be noted that no other instability is theoretically possible under the present experimental condition.

It is known that zero-frequency mode is unstable in counterstreaming ion beams when  $V_b \approx a_b$  though it was not observed here.<sup>7</sup> The reason is that plasma ions which coexist in this experiment stabilize the mode. We estimate the critical density of plasma ions ( $n_{ic}$ ) for the mode to be unstable. The ratio  $\alpha (= n_{ic}/n_e)$  is given by  $2T_b/T_e + 2\alpha T_b/T_i = (1 - \alpha)Z_r'(V_b/a_b)$ , which is obtained from Eq. (1) under the assumption that  $\omega_r = \omega_i = 0$  and  $k^2/k_e^2 \ll 1$ . Considering that the maximum value of  $Z_r'$  is 0.45 and that  $0.1T_e = T_i = T_b$  when  $V_b \approx a_b$ , we obtain  $\alpha = 0.10$ . In the experiment, as  $n_i/n_e$  is about 0.2, in other words, the density of one beam is 40% of electron density, this mode is not unstable.

Heating of beam ions due to the ion-ion instability has been observed experimentally by Taylor and Coroniti.<sup>8</sup> Computer simulation shows that the ion-ion and the electron-ion instabilities in the counterstreaming ion beams are effective in heating of ions.<sup>9</sup> In this experiment, as shown in Fig. 3, the amplitude of oscillation is so large that heating of beam ions is expected. To see heating of beam ions, the analyzer was set in the right source chamber so as not to suffer the influence of oscillation which was almost confined in the target chamber. It measured the beam ions which had originated in the left source chamber, passed the target chamber and entered into the right source. The result was that the ratio of the temperature of beam ions when the oscillation existed to that without oscillation was about 5 when  $V_b/C_s \approx 4$  and  $\delta n/n \approx 0.2$ .

In summary, the electron-ion instability is observed when  $V_b/C_s \geq 3$  in the triple-plasma device. Standing oscillations whose wavelengths are equal to the distance between boundaries divided by an integer and which have antinodes at the boundaries are detected. The instability is strongly excited because the system has a feedback in addition to being linearly unstable; the feedback is caused by the reflected wave and by the coupling between the boundaries. Heating of

beam ions due to the strong instability is observed.

<sup>1</sup>T. Ohnuma and Y. Hatta, *J. Phys. Soc. Jpn.* **21**, 986 (1966); B. D. Fried and A. Y. Wong, *Phys. Fluids* **9**, 1084 (1966).

<sup>2</sup>D. Grésillon and F. Doveil, *Phys. Rev. Lett.* **34**, 77 (1975).

<sup>3</sup>R. Limpacher and K. R. Mackenzie, *Rev. Sci. Instrum.* **44**, 726 (1973); Y. Nakamura, B. H. Quon, and A. Y. Wong, *Phys. Lett.* **53A**, 85 (1975).

<sup>4</sup>Intensity of the spontaneous oscillation scarcely varied when the floating grids were grounded through large

capacitance. It implies that the coupling is not due to grids but due to ion sheaths formed in front of the grids. The in-phase coupling was confirmed by the test-pulse method.

<sup>5</sup>Y. Nakamura, *J. Phys. Soc. Jpn.* **31**, 273 (1971).

<sup>6</sup>H. Tanaka, A. Hirose, and M. Koganei, *Phys. Rev.* **161**, 94 (1967); T. Fujita, T. Ohnuma, and S. Adachi, *Plasma Phys.* **19**, 875 (1977).

<sup>7</sup>R. J. Briggs, *Electron-Stream Interactions with Plasmas* (M.I.T. Press, Cambridge, 1964).

<sup>8</sup>R. J. Taylor and F. V. Coroniti, *Phys. Rev. Lett.* **29**, 34 (1972).

<sup>9</sup>D. W. Forslund and C. R. Shonk, *Phys. Rev. Lett.* **25**, 281 (1970).

## Angle-Dependent Photoionization Cross Sections of Cu

D. Liebowitz, M. Sagurton, J. Colbert, and N. J. Shevchik

*Department of Physics, State University of New York, Stony Brook, New York 11794*

(Received 26 August 1977)

It is shown that the positions of the peaks in the angle-resolved photoemission spectra from a Cu(111) surface for  $h\nu = 11.6$ – $40.8$  eV are predicted reasonably well by the initial-state band structure and a single-plane-wave final state, but the strengths of the peaks are described by atomiclike dipole selection rules.

The free-electron final-state (FEFS) model predicts the positions of the peaks in the angle-resolved photoemission spectra of the noble metals reasonably well for  $h\nu = 11$ – $200$  eV,<sup>1,4</sup> but it does not predict correctly the observed strengths of the peaks.<sup>1,5</sup> Constant matrix elements appear to explain the peak strengths better than plane-wave matrix elements,<sup>1,6,7</sup> but there has been no theoretical justification for them. It has been suggested recently<sup>8</sup> that since the photoionization matrix element is predominantly due to the spherically symmetric atomic potential,<sup>5</sup> its angular behavior ought to be governed by atomiclike dipole selection rules.

In this Letter, we show that the angle-resolved photoemission spectra from a Cu(111) surface for photon energies ranging from 11 to 40 eV can be explained by a FEFS model in which the atomic photoionization cross sections calculated by plane waves are replaced by those based upon atomic dipole selection rules.

In the angle-resolved photoemission experiment, the magnitude of the component of the mo-

mentum of the photoelectron parallel to the smooth surface,  $k_{\parallel}$ , which is conserved as the electron passes from the solid into the vacuum, is given by<sup>9</sup>

$$k_{\parallel} = (2mE/\hbar^2)^{1/2} \sin\theta_e, \quad (1)$$

where  $E$  is the measured kinetic energy of the photoelectron,  $\theta_e$  is the polar angle of emission, and  $m$  is the free-electron mass.

Inside the solid, the energy dispersion of the photoelectron with momentum  $\vec{k}_f$  is

$$E_f(\vec{k}_f) = \hbar^2 k_f^2 / 2m^* = E + W, \quad (2)$$

which yields, in terms of  $k_{\parallel}$ , the component of the momentum perpendicular to the surface

$$k_{\perp} = \{ [2m^*(E+W)/\hbar^2] - k_{\parallel}^2 \}^{1/2}, \quad (3)$$

where  $W$  is the inner potential and  $m^*$  is the effective mass of the internal photoelectron, which is close to, but not necessarily equal to, the mass of the free electron.

Including the finite mean free path of the photoelectron, the photoemission spectrum according to the free-electron final-state model is<sup>10</sup>

$$I(E, \vec{k}_{\parallel}, \vec{\epsilon}) \propto \sum_n \int_{-\infty}^{\infty} \sigma_n(\vec{k}, \vec{\epsilon}) \delta(E_f(\vec{k}_f) - E_n(\vec{k}) - \hbar\omega) [\Gamma^2 + (k_{\perp}' - k_{\perp})^2]^{-1} dk_{\perp}', \quad (4)$$

where  $\vec{k} = \vec{k}_{\parallel} + \vec{k}_{\perp}'$ ,  $\Gamma = (l \cos\theta_i)^{-1}$ ,  $l$  is the mean free path of the photoelectron,  $\theta_i$  is the angle between  $\vec{k}_f$  and the normal to the surface,  $\vec{\epsilon}$  is the direction of the electric field of the photon, and  $\sigma_n(\vec{k}, \vec{\epsilon})$  is